

The IS427 and ISOLDE Collaborations

**Laser spectroscopy and  $\beta$ -NMR measurements of  
short-lived Mg isotopes**

Magdalena Kowalska for the IS 427 collaboration at ISOLDE/CERN

*Institut für Physik, Universität Mainz, D-55099 Mainz, Germany  
present address: CERN, Physics Department, CH-1211 Geneva 23, Switzerland*

Abstract

The feasibility of studying the neutron-rich  $^{29}\text{Mg}$ ,  $^{31}\text{Mg}$ , and  $^{33}\text{Mg}$  isotopes has been demonstrated with the laser and  $\beta$ -NMR spectroscopy setup at ISOLDE/CERN. The values of the magnetic moment and the nuclear spin of  $^{31}\text{Mg}$  are reported and reveal an intruder ground state. This proves the weakening of  $N = 20$  shell gap and places this nucleus inside the so called “island of inversion”. The experimental setup and technique, as well as the results, are presented.

PACS: 21.10.Hw- Spin, parity, and isobaric spin; 21.10.Ky - Electromagnetic moments; 27.30.+t -  $20 \leq A \leq 38$  and 32.10.Fn - Fine and hyperfine structure

*Submitted to Hyperfine Interactions*

## INTRODUCTION

Laser techniques can be very useful not only to investigate properties of atoms as a whole, but even to gain insight into the structure of atomic nuclei by using the hyperfine interaction between the electrons and the nucleus [1]. By probing the ground state properties of radioactive nuclei, such techniques can contribute considerably to our understanding of the nuclear structure. This is especially important in unique regions such as the “island of inversion”, which covers neutron-rich nuclei around  $N = 20$  and  $Z = 12$ , whose properties cannot be explained with the simple nuclear shell model, but indicate a weakening of the  $N = 20$  shell gap between the nuclear  $sd$  and  $fp$  shells [2-5]. The odd- $A$  neutron-rich radioactive Mg isotopes are relevant in this context, since with 12 protons and 17 to 21 neutrons, they lie inside or at the borders of this “island”. They have been recently studied at ISOLDE/CERN by employing the techniques related to collinear laser spectroscopy [6, 7].  $\beta$ -NMR measurements for  $^{29,31}\text{Mg}$  on optically pumped ions reveal their nuclear  $g$ -factors, whereas a combination with measurements of the hyperfine structure allows an unambiguous determination of the ground state nuclear spin and parity. For  $^{31}\text{Mg}$ , the measured spin-parity  $I^\pi = 1/2^+$  implies an intruder ground state and proves the weakening of the  $N = 20$  nuclear shell gap for Mg isotopes.

## EXPERIMENTAL METHOD

Neutron-rich Mg isotopes are produced at the ISOLDE mass separator via fragmentation reactions in a uranium carbide target induced by a 1.4 GeV proton beam (typical intensity of  $3 \times 10^{13}$  protons per pulse, every 2.4 seconds). The produced atoms are then resonantly ionised with pulsed lasers (the RILIS method [8]), accelerated to 60 keV, and guided to the setup for the collinear laser spectroscopy, presented in Fig. 1. The typical intensities at the experimental station are:  $6 \times 10^6$ ,  $2 \times 10^5$ , and  $9 \times 10^3$  ions/s of  $^{29}\text{Mg}^+$ ,  $^{31}\text{Mg}^+$ , and  $^{33}\text{Mg}^+$  (with respective half-lives of 1.3 s, 230 ms, and 90 ms). The above yields and half-lives make these Mg isotopes well suitable for  $\beta$ -asymmetry detection of optical pumping and for  $\beta$ -NMR experiments [4, 7].

The principle of the experimental method used for these short-lived isotopes is the following (Fig. 1): the beam is polarised, implanted into a crystal and  $\beta$  decay electrons are detected. Because the nuclei are polarised, their decay is anisotropic and its asymmetry can

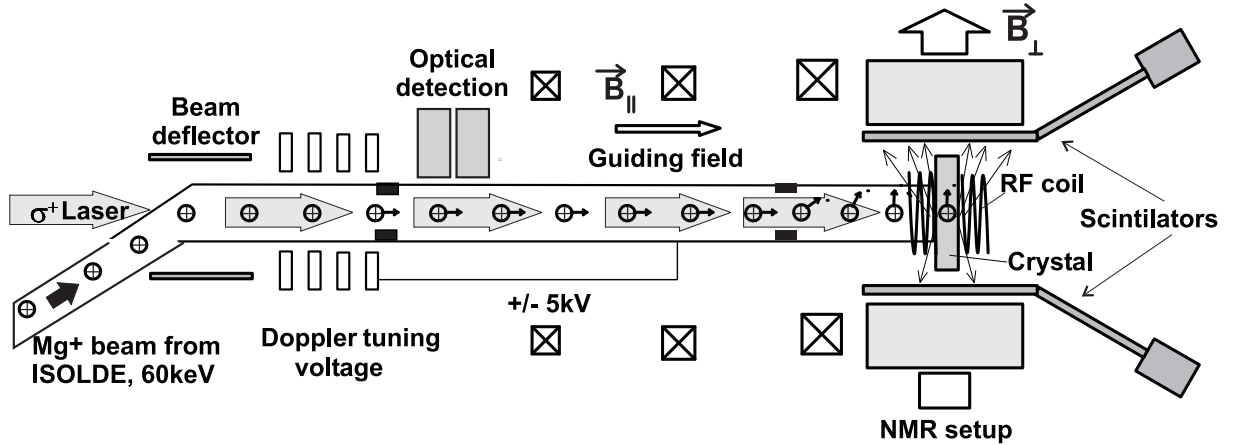


FIG. 1: Experimental setup for laser and  $\beta$ -NMR spectroscopy on Mg ions.

be measured. In the case of Mg beams, the polarization is obtained via optical pumping [4, 9]. For this purpose the ions are overlapped in a weak external magnetic field with circularly polarised laser light, which causes transitions between the Zeeman levels of the hyperfine structure. For magnesium, optical polarization is readily achieved for a singly charged ion in the excitation from the ground state ( $3s^2S_{1/2}$ ) to one of the first excited states,  $3p^2P_{1/2}$  or  $3p^2P_{3/2}$  ( $D_1$  or  $D_2$  line). The principle of the optical pumping is schematically shown in Fig. 2 for  $^{29}\text{Mg}^+$ : in a weak external magnetic field positively polarised light ( $\sigma^+$ ) induces atomic transitions with  $\Delta m_F = +1$  (for  $\sigma^-$ ,  $\Delta m_F = -1$ ). Although the decay is isotropic and  $\Delta m_F = -1, 0$  or  $+1$ , the laser light interacts many times with the same atom and causes excitations in which  $m_F$  can only increase by 1 (decreases by 1 for  $\sigma^-$ ). As a result, most of Mg ions are in the ground state substate with the highest  $m_F$  (for  $\sigma^+$ , or lowest  $m_F$  for  $\sigma^-$ ). A complication to this quite straightforward process is caused by the hyperfine pumping, in which the excited state decays to the other ground state level ( $F = 1$  in Fig. 2). This lowers the population of the ground state component available for optical pumping and therefore the polarization is not equal to 100% [4].

The problem of efficient optical pumping is the laser power. The ultraviolet transition wavelength, 280 nm, was produced by the frequency doubling of visible dye laser radiation. The best doubling efficiency is obtained by an external resonator, therefore the experimental challenge is the setting and operation of a relatively complicated and delicate laser system for an online experiment. The fundamental beam is produced in a ring dye laser (Pyromethene 556 as the active medium) pumped by a multiline  $\text{Ar}^+$  laser. Powers up to 1 W at 560 nm were obtained with 6 W pumping. The output is then frequency doubled in an external

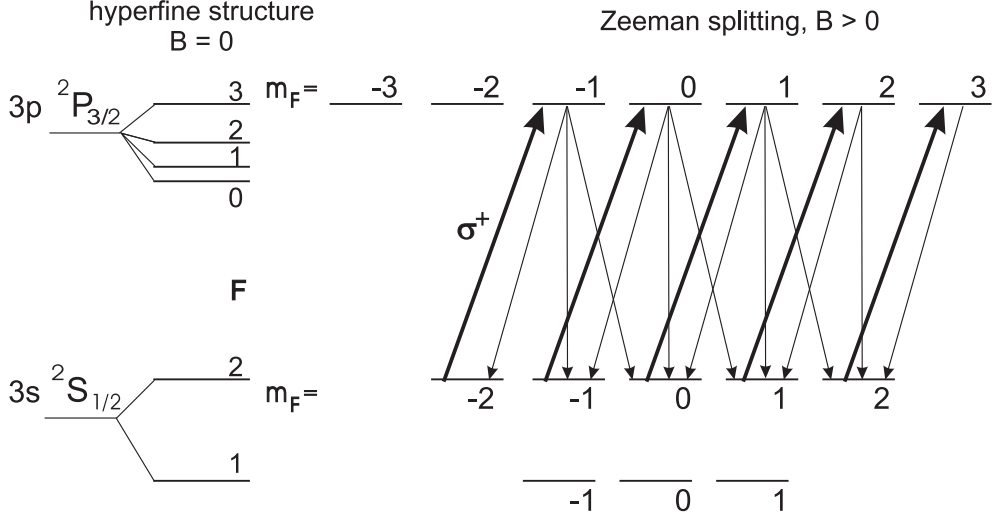


FIG. 2: Optical pumping with  $\sigma^+$  light for the  $D_2$  line of  $^{29}\text{Mg}^+$  ( $I = 3/2$ ,  $\mu_I > 0$ ).

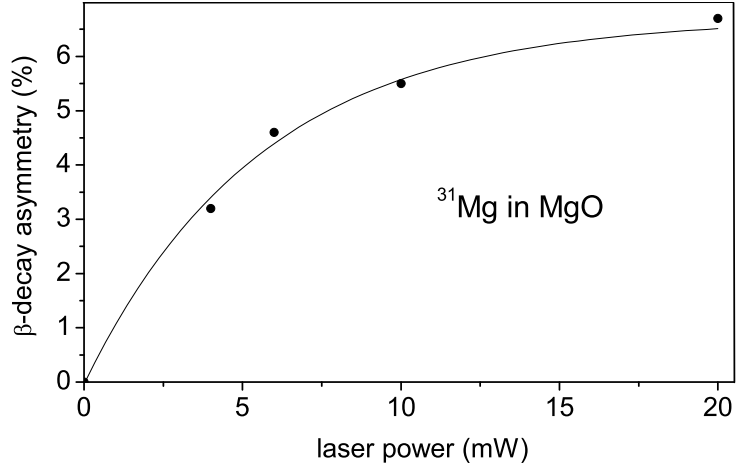


FIG. 3:  $\beta$ -decay asymmetry as function of laser power. The polarization achieved at 20 mW is close to saturation.

*DeltaConcept* resonator with a BBO crystal and angle tuned phase-matching, and UV powers up to 15-20 mW are reached. Measurements with different laser powers show that the polarization achieved by optical pumping is close to saturation (Fig. 3).

Optical pumping creates longitudinal polarization of the total (electronic and nuclear) spin system. Mg ions move further to a region of gradually increasing magnetic field, where the spins are adiabatically rotated and then decoupled, before entering a high transverse magnetic field (about 0.3 T) of an NMR-magnet. The ions are implanted into a crystal located in the middle of the magnet and their  $\beta$  decay is observed in a pair of plastic scintillators placed at  $0^\circ$  and  $180^\circ$  with respect to the magnetic field. Since  $\beta$  decay of a

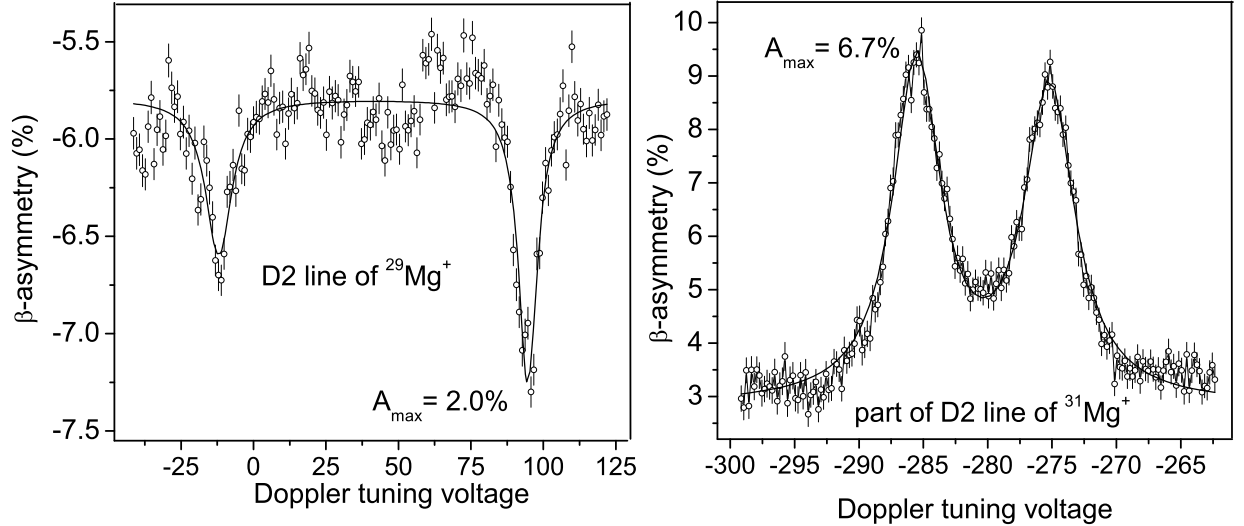


FIG. 4: The experimental  $\beta$ -asymmetries in the  $D_2$  line of  $^{29}\text{Mg}^+$  and  $^{31}\text{Mg}^+$  as a function of Doppler tuning voltage.

polarised ensemble is not isotropic, the amount of nuclear polarization created via optical pumping is reflected in the experimental asymmetry, expressed as  $A = (N_1 - N_2)/(N_1 + N_2)$ , with  $N_1$  and  $N_2$  as  $\beta$  counts in the detectors.

One of the advantages of working with ions is the possibility that, instead of changing the laser frequency  $\nu_L$  (requiring a relatively complicated calibration of the laser wavelength), one can modify the velocity of the ions. For this purpose the optical pumping section forms a Faraday cage at a variable electrical potential  $U$  (Fig. 1), which produces a Doppler shift of the laser frequency in the rest frame of the ions. The approach is known as “Doppler tuning” [10] and the frequency  $\nu$  in the frame of the ion is described by the following relation:  $\nu = \nu_L(1 - \beta)/\sqrt{(1 - \beta^2)}$ , where  $\beta = v/c = \sqrt{1 - (1 + b)^{-2}}$  and  $b = eU/mc^2$  (with the electric charge  $e$ , velocity of light  $c$ , and rest mass of the ion  $m$ ). In the first step, this “Doppler tuning” is used to record the hyperfine structure, which is observed in the change of the  $\beta$  asymmetry as a function of the acceleration voltage (Fig. 4). From these measurements  $A$  and  $B$  hyperfine constants may be deduced, which in turn reveal the nuclear magnetic and quadrupole moments. (In the case of the Mg ion, from the two lines used in this experiment, only the transition to the  $^2P_{3/2}$  level can reveal the quadrupole moment, but because the hyperfine components of this state are not very well resolved, it is hard to obtain accurate information about the quadrupole moment in this way). After a hyperfine structure scan, the acceleration voltage is fixed at the hyperfine component giving

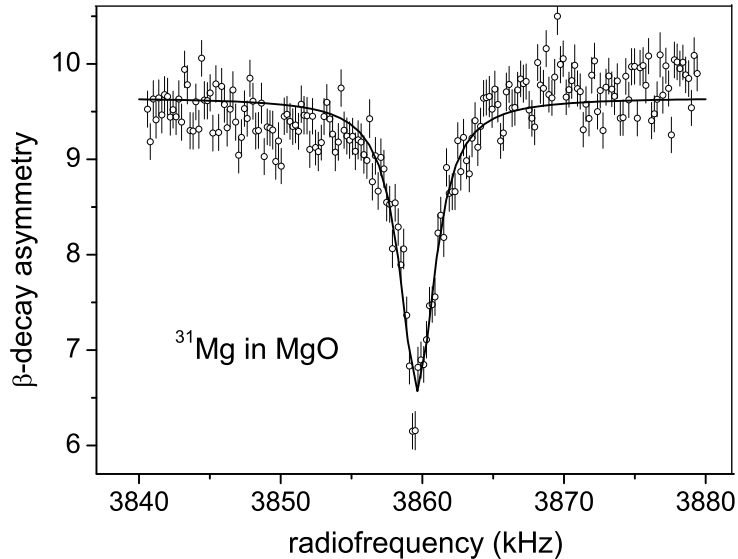


FIG. 5: Typical  $\beta$ -NMR resonance of  $^{31}\text{Mg}$  implanted in MgO.

largest asymmetry and NMR scans are performed: a radio-frequency field is produced by a coil placed around the host crystal, and when the frequency corresponds to the spacing  $\Delta E_{mag}$  between different  $m_I$  substates of the studied nucleus, transitions between these levels occur. The redistribution of the  $m_I$  substates reduces the nuclear polarization, seen in the disappearance of the experimental asymmetry. If a cubic host crystal is chosen, the resonance radio-frequency corresponds to the Larmor frequency, given by  $\Delta E_{mag} = \nu_L h = g_I \mu_N B$  (with the nuclear  $g$ -factor  $g_I$ , nuclear magneton  $\mu_N$  and external magnetic field  $B$ ). For non-cubic host crystals, the resonance at the Larmor frequency is symmetrically split in  $2I$  components by the interaction of the quadrupole moment  $Q_S$  with the internal electric field gradient  $V_{zz}$ , with the splitting proportional to  $Q_S V_{zz}$ . In this way, very accurate measurements of the nuclear magnetic and quadrupole moments can be performed.

## EXPERIMENTAL RESULTS

The first measurements on Mg beams were performed to test the optical polarization for  $^{29}\text{Mg}^+$  and  $^{31}\text{Mg}^+$ . For this purpose different cubic host crystals were used. MgO gave the highest asymmetries at room temperature (up to 6.7% for  $^{31}\text{Mg}$  in the  $D_2$  line) and was used in the experiments. The other tested crystals were Pt and Au, giving 3.1% and 1.8% asymmetry (also for  $^{31}\text{Mg}$ ), respectively. These tests showed that optical pumping experiments with Mg beams provided by ISOLDE are feasible (Fig. 4).

After hyperfine scans, NMR measurements in MgO followed for both  $^{29}\text{Mg}$  and  $^{31}\text{Mg}$ . At

the time of the workshop (May 2004) their analysis was still in progress, therefore no results were presented. This analysis has been now completed for  $^{31}\text{Mg}$  and is published [11]. A brief summary of the results is presented below.

The highlights of these measurements are the ground state properties of  $^{31}\text{Mg}$ , especially the unknown nuclear spin. By  $\beta$ -NMR we determined the nuclear  $g$ -factor. Calibration of the magnetic field was performed on  $^8\text{Li}$  ( $g(^8\text{Li}) = 0.826780(9)$  [12]) available from the same ISOLDE target, and it yields  $\nu_L(^8\text{Li}) = 1807.03(2)$  kHz. Measurements on  $^{31}\text{Mg}$  give  $\nu_L(^{31}\text{Mg}) = 3859.73(18)$  kHz (Fig. 5). The resulting value of the  $g$ -factor of  $^{31}\text{Mg}$  (corrected for diamagnetism) is thus  $|g| = 1.7671(3)$  [11]. The final error includes a systematic uncertainty accounting for the inhomogeneities of the magnetic field and its drift between the measurements on  $^{31}\text{Mg}$  and  $^8\text{Li}$ .

The magnitude of the hyperfine splitting is proportional to the product of  $g$  and  $I$  (and the position of particular components depends on the sign of  $g$ ). By combining the NMR and hyperfine results we are able to determine the spin and parity of  $^{31}\text{Mg}$  ground state to be  $1/2^+$  [11]. This result requires at least 2 neutrons in the  $fp$  shell, which shows the intruder character of the ground state and proves the weakening of the  $N = 20$  shell gap.

Future plans include measurements of the magnetic and quadrupole moment of  $^{33}\text{Mg}$ , as well as isotope shifts between different neutron-rich isotopes of magnesium.

This work was supported by the German Ministry for Education and Research (BMBF) under contract no. 06MZ175, by the IUAP project no. p5-07 of OSCT Belgium, by the FWO-Vlaanderen under the Grant-in-Aid for Specially Promoted Research (no. 13002001) and the EU under EURONS project (no. 506065). The authors thank the ISOLDE technical group for their assistance during the experiment.

- 
- [1] R. Neugart, Eur. Phys. J. A 15, 35 (2002).
  - [2] C. Thibault *et al.*, Phys. Rev. C 12, 644 (1975).
  - [3] C. Detraz *et al.*, Phys. Rev. C 19, 164 (1979).
  - [4] M. Keim *et al.*, Eur. Phys. J. A 8, 31 (2000).
  - [5] D. Guillemaud-Mueller *et al.*, Nucl. Phys. A 426, 37 (1984).
  - [6] R. Neugart, Nucl. Inst. Meth. 186, 165 (1981).
  - [7] W. Geithner *et al.*, Phys. Rev. Lett. 83, 3792 (1999).
  - [8] U. Köster *et al.*, Nucl. Instr. Meth. B 204, 347 (2003).
  - [9] E. Arnold *et al.*, Phys. Lett. B 197, 311 (1987).
  - [10] S. L. Kaufman, Opt. Comm. 17, 309 (1976).
  - [11] G. Neyens *et al.*, Phys. Rev. Lett. 94, 22501 (2005).
  - [12] P. Raghavan, At. Data Nucl. Data Tables 42, 189 (1989).